^{3}He and ^{4}He production by 800 MeV protons from ^{12}C, Ti, and Pb at forward angles

D. B. Barlow,* B. M. K. Nefkens, C. Pillai,* J. W. Price, I. Šlaus,† M. J. Wang, and J. A. Wightman‡
University of California, Los Angeles, California 90024

K. W. Jones, M. J. Leitch, C. S. Mishra, C. L. Morris, and J-C Peng
Los Alamos National Laboratory, Los Alamos, New Mexico 87545

P. K. Teng
Institute of Physics, Academia Sinica, Nankang, Taiwan

J. M. Tinsley
Arizona State University, Tempe, Arizona 85281
(Received 10 September 1991)

The doubly differential cross section for the production of ^{3}He and ^{4}He by 800 MeV protons from ^{12}C, Ti, and Pb has been measured at laboratory angles of 6° and 15°. The momentum of the detected helium nuclei varied from 1 to 2 GeV/c, the maximum being well above the incident proton momentum of 1.46 GeV/c. The cross sections were found to increase with increasing target mass and decrease with increasing momentum and scattering angle. In our momentum region, the ^{3}He production cross section is 1.5–10 times larger than ^{4}He depending on the target and the momentum. The data are consistent with the hypothesis that the dominant reaction mechanism is a direct process where the initial nucleon-nucleon scattering is followed by a sequential pickup of neutrons.

PACS number(s): 25.40.Hs, 27.20.+n, 27.40.+z, 27.80.+w

I. INTRODUCTION

The production of nuclear fragments by intermediate and high-energy protons and by light and heavy ions interacting with complex nuclei has been under investigation for over three decades [1,2]. When a very energetic projectile interacts with a target nucleus, a great number of final states are available. A large fraction of the cross section comes from the emission of particles with more than 10 MeV/nucleon. Inclusive spectra of fragments produced in the proton bombardment of targets ranging from Be to Pb show a sharp decrease with increasing fragment energy, indicative of an evaporation process. Evaporation explains only the low-energy part of the spectra, and it does not work well for all fragments. It has been shown [3] that in a proton-Ag interaction at 480 MeV at forward angles (20°), the evaporation process contributes 57% of the ^{4}He and only 6% of the ^{3}He emission cross section. The relative contribution of the evaporation process changes with angle, and at 90° it amounts to 76% for ^{4}He and 17% for ^{3}He emission.

Several models, based on a variety of different assumptions, have been proposed to explain light fragment inclusive energy spectra [2]. Neither single nucleon-cluster scattering from a zero-temperature Fermi gas nor emission from an ensemble of particles in thermal equilibrium can account for all observables in the nuclear fragment production. General similarities of fragment production from targets as varying as Be and Ag suggest that the reactions proceed through similar channels in all nuclei; the fragments appear to be emitted from a hot source generated as a result of an initial nucleon-nucleon quasi-free scattering and subsequent final-state interactions [4]. In the present work, the momentum range of the ejectiles, which extends to 1.8 GeV/c for the carbon target and 2.0 GeV/c for the lead target, extends well beyond the incident proton momentum of 1.46 GeV/c. This requires a major contribution coming from the Fermi momentum of the target nucleus and/or the production of backward-going mesons.

The present study was prompted by our desire to know the background ^{4}He production from the titanium in a solid titanium tritide target that is bombarded by 800 MeV protons. It is possible to produce a beam of η mesons from such a target by the reaction $p+{}^{3}\mathrm{H}\rightarrow{}^{4}\mathrm{He}+\eta$. The recoil ^{4}He serves for tagging the η using the constraints of two-body kinematics [5]. The most interesting energy region is near the η production threshold ($T_p=756$ MeV), as the Jacobian of the ^{4}He is the largest at threshold and the laboratory differential cross section for η production is at its peak, assuming that the η production process is similar to the one in $p+d\rightarrow{}^{3}\mathrm{He}+\eta$ [6]. Threshold production implies that the ^{4}He emerges near 0° in the laboratory system with

*Present address: Los Alamos National Laboratory, Los Alamos, NM 87545.

†Permanent address: Ruđer Bošković Institute, Zagreb, Croatia, Yugoslavia.

‡Present address: Dept. of Physics, Texas A&M Univ., College Station, TX 77843 and Texas Accelerator Center, The Woodlands, TX 77381.

momentum $p_\alpha = 1.3$ GeV/c. The titanium in the Ti(^{3}H)$_2$ target under consideration weights considerably more than the tritium and could provide a prohibitively large background. Hence it is important to know the magnitude of ^{4}He production from the background material.

We have embarked on a short program for measuring ^{4}He production in the range 1–2 GeV/c near 0° when titanium is bombarded by 800 MeV protons. Our study also includes measurements of ^{3}He inclusive energy spectra. Both ^{3}He and ^{4}He spectra are measured for a light (^{12}C) medium (Ti) and heavy (Pb) target. This enables us to explore the A dependence of ^{4}He and ^{3}He production to optimize the choice of alternative target materials in eta meson production experiments. It also provides useful tests on different nuclear fragmentation models.

II. EXPERIMENTAL SETUP

The experiment was performed at the Los Alamos Meson Physics Facility (LAMPF) using the high resolution spectrometer (HRS) [7]. The incident proton beam had a kinetic energy of 800 MeV and the intensity was ~1 nA. The three targets were ^{12}C (500 gm/cm^2), natural Ti (700 mg/cm^2), and natural Pb (200 mg/cm^2). Natural titanium contains 73.8% ^{48}Ti, 8.0% ^{46}Ti, 7.3% ^{47}Ti, 5.5% ^{49}Ti, and 5.4% ^{50}Ti, and natural lead contains 52.4% ^{208}Pb, 24.1% ^{206}Pb, 22.1% ^{207}Pb, and 1.4% ^{204}Pb. The forward-going ^{3}He and ^{4}He produced in the target were bent 150° vertically by the HRS spectrometer magnet and detected in the focal plane. Because of the high rate of background particles such as pions, protons, and deuterons which are copiously produced at forward angles, the HRS focal plane drift chambers were not used. Instead, the ^{3}He and ^{4}He were detected and identified using a pair of scintillation counters spaced ~70 cm apart. This was sufficient to identify particles cleanly by time of flight and pulse height (see Fig. 1). During data acquisition, the scintillator thresholds were set to reject $A<3$ particles from the event trigger. The particle momentum was determined by the field setting of the two spectrometer dipoles. The momentum bite of the HRS spectrometer here is 3%. The absolute calibration of the spectrometer was determined by measuring the cross section for P-C and p-Pb elastic scattering and comparing to known results [8]. From this calibration, the absolute cross sections are known to ±10%.

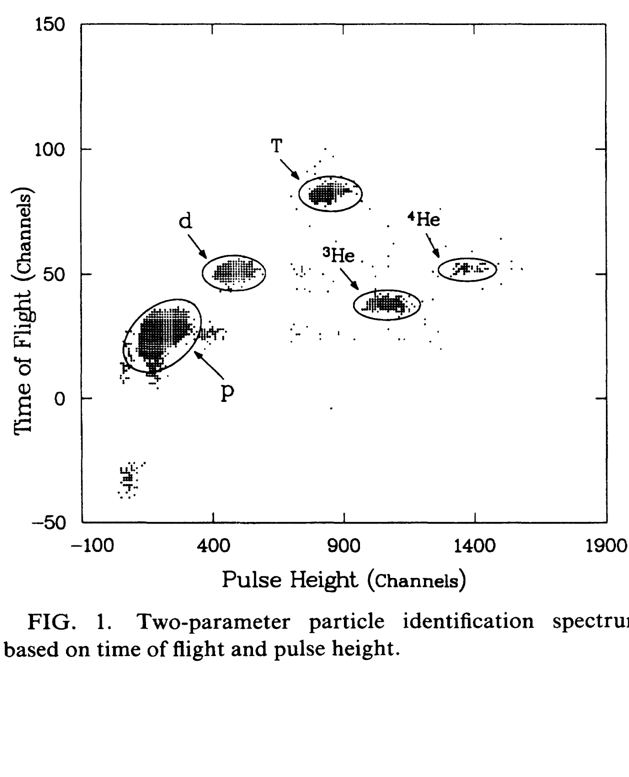

FIG. 1. Two-parameter particle identification spectrum based on time of flight and pulse height.

III. RESULTS AND DISCUSSION

The measured doubly differential cross sections for ^{3}He and ^{4}He production from the carbon, titanium, and lead targets at the laboratory angle of 6° are shown in Tables I–IV and in Figs. 2 and 3. The cross sections from Ti at the laboratory angle of 15° are given in Fig. 4. A small adjustment was made to the measured momentum to account for the average energy loss of the outgoing particles from the target. The statistical errors are approximately the size of the data points.

The maximum value of the ejectiles' momentum is 2 GeV/c, well above the incident proton momentum of 1.46 GeV/c. As expected, the cross sections increase with increasing target mass and decrease with increasing ejectile momentum and laboratory angle. The cross section for ^{3}He is almost flat at lower momenta in the energy region displayed in Fig. 3 and it is 2–6 times larger than the ^{4}He cross section (Fig. 2). It is known that, although the total (p,α) cross section is about ten times larger than the total $(p,{}^3\text{He})$ cross section, the cross section for ^{3}He emission is larger than that for ^{4}He, for fragment energies larger than about 100 MeV [1,9].

Larger differences in evaporation probabilities for ^{4}He and ^{3}He are expected and found. Evaporation is strongly dependent on the isotope of the ejectile, reflecting the relative separation energies. In general, inclusive energy spectra have much lower slopes in the high-energy region for neutron deficient isotopes; for example, ^{7}Be (and similarly ^{10}C and ^{11}C) inclusive energy spectra decrease as the energy increases much more slowly than spectra of ^{9}Be and ^{12}C ejectiles. It is argued that the neutron-deficient

TABLE I. Doubly differential cross sections for ^{3}He and ^{4}He production by 1.46 GeV/c protons at 6° (lab) on a ^{12}C target. Only statistical errors are quoted. Systematic errors are ±10%.

$p(^3\text{He})$ (GeV/c)	$\frac{d^2\sigma}{dp\,d\Omega}$ [μb/(sr MeV/c)]	$p(^4\text{He})$ (GeV/c)	$\frac{d^2\sigma}{dp\,d\Omega}$ [μb/(sr MeV/c)]
1.02	0.316±0.003	1.06	0.076±0.001
1.22	0.300±0.003	1.24	0.051±0.001
1.30	0.330±0.002	1.32	0.048±0.001
1.33	0.311±0.003	1.35	0.043±0.001
1.36	0.300±0.003	1.38	0.040±0.001
1.39	0.306±0.003	1.41	0.037±0.001
1.42	0.310±0.003	1.43	0.034±0.001
1.45	0.288±0.003	1.46	0.029±0.001
1.51	0.280±0.003	1.53	0.026±0.001
1.63	0.200±0.002	1.65	0.018±0.001
1.75	0.140±0.002	1.76	0.014±0.001
1.85	0.051±0.001	1.86	0.007±0.001
1.95	0.030±0.001	1.96	0.004±0.001

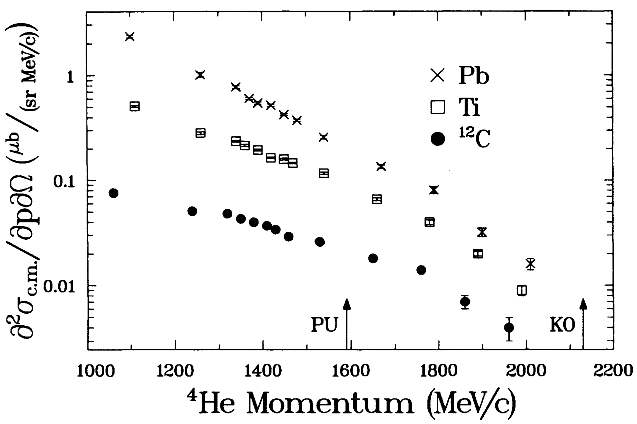

FIG. 2. Doubly differential cross sections in the c.m. for the production of ^{4}He from the ^{12}C, Ti, and Pb by 800 MeV (1460 MeV/c) protons at 6°. Arrows labeled KO and PU indicate kinematic conditions for the knockout and pickup processes described in the text.

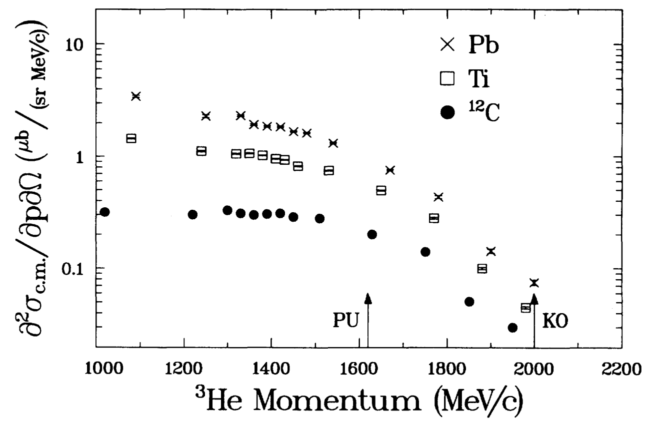

FIG. 3. Doubly differential center-of-mass cross sections for the production of ^{3}He from ^{12}C, Ti, and Pb by 800 MeV (1460 MeV/c) protons at 6°. Arrows labeled KO and PU indicate kinematic conditions for the knockout and pickup processes described in the text.

isotopes are produced from sources in nuclei which are excited to higher temperature [1,9].

The measurement of the linear momentum transferred from projectile to the emitted nucleus in a given nuclear interaction provides insight in the reaction mechanism. Several processes are possible and most likely all occur to some extent simultaneously. We will now investigate some of these mechanisms.

The emission cross section for ^{3}He and ^{4}He resulting from the 800 MeV proton bombardment of a natural Ti target is peaked in the forward direction (compare the data in Figs. 2 and 3 with those of Fig. 4), providing support for the earlier measurements in the 20°–170° region [1]. Specifically, the more energetic ^{3}He ($p \geq 1700$ MeV/c) emission cross section at 6° is about three times larger than at 15°. However, for lower-energy ^{3}He (1100 MeV/c), the 6° and 15° cross sections are about equal.

The high momentum region of the inclusive ^{3}He and ^{4}He spectra could be due to the direct knockout (KO) of a preformed cluster of ^{3}He or ^{4}He by the incident proton regardless of the details of the proton-cluster interaction process. Assuming free and stationary ^{3}He and ^{4}He clusters, one obtains for the ejected particle momenta values denoted by the KO arrow in Figs. 2–4. The cross sections for these processes are proportional to the product of the probability for the ^{4}He or ^{3}He cluster formation, the $p-{}^3$He (and p-α) cross section, and the probability that the cluster will escape and not rescatter or break up after it is struck by the incident proton. The experimental spectra (Figs. 2–4) do not support the hypothesis that the cross sections for ^{4}He and ^{3}He are due to knockout. This is in accord with other available data (see, e.g., Ref. 2). The knockout occurs mainly in the surface of the target nucleus and one expects that the cross sections for ^{12}C, Ti, and Pb behave as $A^{2/3}$. We have investigated the A dependence of the ^{3}He and ^{4}He emission cross sections and its variation with the ejectile momentum as follows.

The doubly differential cross sections are fitted with a function of the form

TABLE II. Doubly differential cross sections for ^{3}He and ^{4}He production by 1.46 GeV/c protons at 6° (lab) on a Ti target. Only statistical errors are quoted. Systematic errors are ± 10%

$p(^3\text{He})$ (GeV/c)	$\frac{d^2\sigma}{dp\,d\Omega}$ [μb/(sr MeV/c)]	$p(^4\text{He})$ (GeV/c)	$\frac{d^2\sigma}{dp\,d\Omega}$ [μb/(sr MeV/c)]
1.08	1.449±0.015	1.11	0.511±0.009
1.24	1.115±0.016	1.26	0.283±0.008
1.32	1.058±0.011	1.34	0.236±0.004
1.35	1.065±0.011	1.36	0.215±0.005
1.38	1.023±0.010	1.39	0.195±0.004
1.41	0.954±0.009	1.42	0.164±0.003
1.43	0.935±0.009	1.45	0.159±0.003
1.46	0.821±0.008	1.47	0.146±0.002
1.53	0.750±0.007	1.54	0.117±0.003
1.65	0.496±0.005	1.66	0.066±0.002
1.77	0.280±0.005	1.78	0.040±0.002
1.88	0.100±0.002	1.89	0.020±0.001
1.98	0.045±0.001	1.99	0.009±0.001

TABLE III. Doubly differential cross sections for ^{3}He and ^{4}He production by 1.46 GeV/c protons at 6° (lab) on a Pb target. Only statistical errors are quoted. Systematic errors are ± 10%.

$p(^3\text{He})$ (GeV/c)	$\frac{d^2\sigma}{dp\,d\Omega}$ [μb/(sr MeV/c)]	$p(^4\text{He})$ (GeV/c)	$\frac{d^2\sigma}{dp\,d\Omega}$ [μb/(sr MeV/c)]
1.09	3.45±0.07	1.10	2.33±0.06
1.25	2.31±0.07	1.26	1.01±0.05
1.33	2.34±0.04	1.34	0.774±0.025
1.36	1.94±0.03	1.37	0.603±0.016
1.39	1.87±0.03	1.39	0.547±0.014
1.42	1.85±0.03	1.42	0.521±0.014
1.45	1.68±0.02	1.45	0.424±0.009
1.48	1.63±0.02	1.48	0.375±0.011
1.54	1.32±0.02	1.54	0.259±0.009
1.67	0.755±0.011	1.67	0.135±0.005
1.78	0.432±0.013	1.79	0.081±0.006
1.90	0.142±0.006	1.90	0.032±0.003
2.00	0.075±0.004	2.01	0.016±0.002

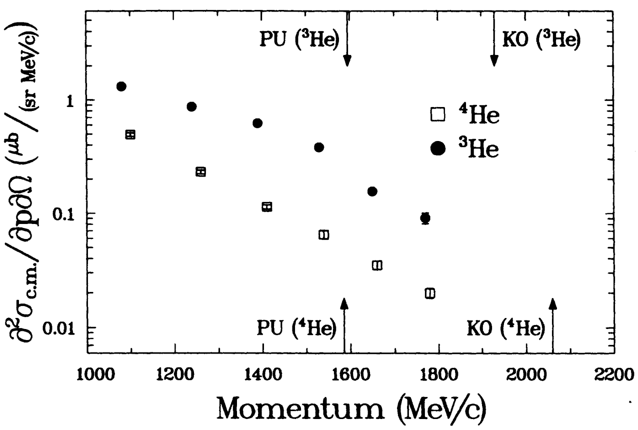

FIG. 4. Doubly differential center-of-mass cross sections for the production of ^{3}He and ^{4}He from Ti by 800 MeV protons (1460 MeV/c) at 15°. Arrows labeled KO and PU indicate kinematic conditions for the knockout and pickup processes described in the text.

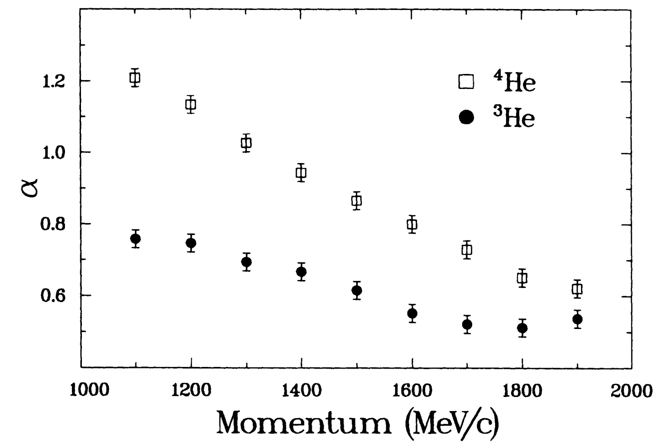

FIG. 5. Variation of the A dependence of the ^{3}He and ^{4}He emission cross sections as a function of the momentum of the ejectiles. The doubly differential cross section $d^2\sigma/(dp\,d\Omega)$ data at 6° laboratory angle, have been fitted with the function CA^{α}. A plot of α as a function of the momentum of the ejectiles is shown.

$$\frac{d^2\sigma}{dp\,d\Omega}=CA^{\alpha} ,$$

where the doubly differential cross section is given in μb/(sr MeV/c, p is the momentum in MeV/c, and A is the atomic number of the target nucleus. The two constants C and α were determined by a simple search for the minimum χ^2. General weighting, using a 10% error, was used in the calculation. (The result for α is not very sensitive to how big the error is.) Since the differential cross section was not measured at the same momenta for the three different targets, they were evaluated every 100 MeV/c from 1100 to 1900 MeV/c by interpolation using a smooth curve drawn by eye through the measured points. The error in α was estimated assuming a 5% random error in each measurement. This error is about 0.025 for all points. A plot of α vs p for ^{3}He and ^{4}He is shown in Fig. 5.

For large momenta (1700–200 MeV/c) the cross sections for both ^{3}He and ^{4}He for ^{12}C, Ti, and Pb behave approximately as $A^{2/3}$. For lower momenta, the cross sections behave as A^{α} with α increasing as the momentum decreases; for ^{3}He from $\alpha=0.55$ to 0.76 and for ^{4}He from $\alpha=0.63$ to 1.2. This momentum variation of the A dependence confirms that the high momentum region is

TABLE IV. Doubly differential cross sections for ^{3}He and ^{4}He production by 1.46 GeV/c protons at 15° (lab) on a Ti target. Only statistical errors are quoted. Systematic errors are ± 10%.

$p(^3\text{He})$ (GeV/c)	$\frac{d^2\sigma}{dp\,d\Omega}$ [μb/(sr MeV/c)]	$p(^4\text{He})$ (GeV/c)	$\frac{d^2\sigma}{dp\,d\Omega}$ [μb/(sr MeV/c)]
1.08	1.32±0.03	1.10	0.494±0.019
1.24	0.868±0.019	1.26	0.231±0.009
1.39	0.621±0.013	1.41	0.114±0.005
1.53	0.38±0.02	1.54	0.065±0.005
1.65	0.156±0.006	1.66	0.035±0.003
1.77	0.091±0.01	1.78	0.020±0.002

dominated by processes in the surface, while at lower momenta the reaction mechanism is more complex and most of the nucleus is involved in the reaction process. The $A^{2/3}$ dependence does not prove that the process is the knockout process. Indeed, if it would be only a knockout process and assuming that the number of ^{3}He and ^{4}He clusters in the surface is about equal, one would expect about equal $(p,^3\text{He})$ and (p,α) cross sections. However, we observe that the $(p,^3\text{He})$ cross section is about six times larger than (p,α). We conclude that at 800 MeV the knockout mechanism is not important and that even the largest momentum region of the inclusive ^{3}He and ^{4}He spectra is due to other peripheral processes with an $A^{2/3}$ dependence.

For incident protons of about 1 GeV, the proton-nucleus interaction is dominated by a series of nucleon-nucleon interactions initiating a nuclear cascade. The similarity between the proton, deuteron, triton, and ^{3}He emission spectra in the high momentum region suggests the importance of the pickup model [1]. The simple pickup model has been considerably improved and developed into a fairly sophisticated one called the snowball model [2,10]. We will use it here in its simplest form. In our case, a proton picks up a neutron and forms a deuteron through the reaction

$$p+n\rightarrow d+\pi^0 . \qquad (1a)$$

This deuteron subsequently picks up another proton and forms ^{3}He via

$$d+p\rightarrow {}^3\text{He}+\pi^0 . \qquad (1b)$$

In the energy region relevant for our data, a significant fraction of the nucleon-nucleon total cross section is due to pion production. Indeed, at 730 MeV, charged pion production on a ^{1}H or a ^{2}H target has a doubly differential cross section of several μb/sr MeV [11]. Alternative pickup processes leading to ^{3}He are

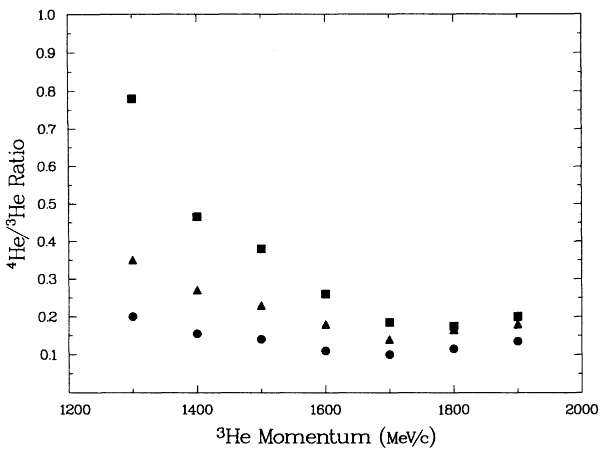

FIG. 6. Ratio of the ^{3}He and ^{4}He production cross sections at p_3 and p_4, which are defined in the text. Solid circles are ^{12}C data, triangles are Ti data, and squares are Pb data.

$$p+p \to d+\pi^+ , \quad (1c)$$

followed by (1b). This accounts for the production of a ^{3}He nucleus.

The largest ^{3}He momentum which these sequential pickup processes can produce at 6° is 1.6 GeV/c (see the arrow PU in Fig. 3). However, the Fermi motion in the nucleus extends the pickup mechanism to considerably larger momenta of the ^{3}He. Figure 3 shows that the inclusive energy spectra of ^{3}He ejectiles from ^{12}C, Ti, and Pb are rather flat below about 1.6 GeV/c.

One more pickup process, $^3\text{He}+n \to \alpha+\pi^0$, or $^3\text{He}+p \to \alpha+\pi^+$, forms ^{4}He. At ^{3}He momenta below 1.6 GeV/c, these pickup processes occur only when the Fermi momenta are 0.1 GeV/c (for 1.5 GeV/c ^{3}He) to 0.2 GeV/c (for 1.1 GeV/c ^{3}He).

Another sequential pickup process would be a pickup of preformed clusters of deuterons (or ^{3}H) to from ^{3}He (or ^{4}He). In our energy region such processes are orders of magnitude less probable. The simple pickup mechanism can be extended to include other possible processes [2], for example, an incident proton scatters sequentially from several nucleons which later coalesce into ^{3}He or ^{4}He. We are neglecting such processes, since we are concerned with the very forward part of the angular distribution; after the first scattering at 6°, the recoil proton leaves at the large angle of 81.5° with a very low energy of 12.4 MeV. Since the ^{3}He production cross section is about five times larger than that of ^{4}He, the dominant processes are sequential pickup mechanisms (1a–c) rather than the pickup of preformed d or t clusters, as the number of preformed deuteron clusters cannot be an order of magnitude larger than the number of triton clusters.

If sequential pickup is the dominant mechanism, then the ratio of the cross sections for ^{3}He and ^{4}He production is proportional to the cross section for neutron pickup by ^{3}He:

$$\sigma(\alpha,p_4)/\sigma(^3\text{He},p_3)=A\,\sigma(^3\text{He}+n \to {}^4\text{He}+\pi^0;p_3,p_4) , \quad (2)$$

where $\sigma(\alpha,p_4)$ and $\sigma(^3\text{He},p_3)$ are production cross sections for ^{4}He and ^{3}He having momenta p_4 and p_3, respectively, and $\sigma(^3\text{He}+n \to \alpha+\pi^0;p_3,p_4)$ is the cross section for neutron pickup by ^{3}He with momentum p_3, while the ^{4}He has momentum p_4. A has a dimension of (length)$^{-2}$. If this model is adequate, then the ratio of the ^{3}He and ^{4}He production cross sections at p_3 and p_4, respectively, is a slowly varying function of p_3, since in this energy region the pickup cross section $\sigma(^3\text{He}+n \to \alpha+\pi^0)$ does not vary rapidly with energy. The difference between p_3 and p_4 in the sequential pickup mechanism varies from about 0 at 1800 MeV/c to about 180 MeV/c at 1100 MeV/c. These are average values of p_3-p_4, since the pickup can occur at all angles. The smooth variation of the ratio (2) with p_3 supports the conjecture that the sequential pickup mechanism (1a–1c) is the dominant process, see Fig. 6. This is further corroborated by the fact that the ratio (2) depends on the target as $A^{1/3}$; the larger the diameter of the target, the more likely it is for ^{3}He to pick up a neutron to form ^{4}He.

IV. CONCLUSION

The production of energetic (1–2 GeV/c) ^{3}He at 6° to 15° laboratory angles is greater than that of ^{4}He; for ejectiles with $p=1.1-1.5$ GeV/c the ^{3}He/^{4}He ratio is 1.5–5 and for $p>1.5$ GeV/c it is 4.5–10. This is markedly different from the part of the spectra where the boiloff mechanism dominates and where the ^{4}He yield exceeds ^{3}He by a factor of 10 and more. The ^{3}He/^{4}He ratio is larger for a light nucleus ^{12}C(5–10 times) than for the heavier nuclei Ti (4–7 times) and Pb (1.5–5 times). Our data are consistent with the assumption that the dominant mechanism is the sequential pickup (1a–1c) mechanism.

ACKNOWLEDGMENTS

It is a pleasure to thank R. Korteling and V. Viola for some informative comments on light fragment emission. This work was supported in part by the U.S. DOE.

[1] A. M. Poskanzer, A. W. Butler, and E. K. Hyde, Phys. Rev. C **3** 882 (1971); V. T. Cocconi *et al.*, Phys. Rev. Lett. **5**, 19 (1960); V. L. Fitch *et al.*, Phys. Rev. **126**, 1849 (1962); R. A. Korteling, C. R. Torren, and E. K. Hyde, Phys. Rev. C **7**, 1611 (1973); J. R. Wu, C. C. Chang, and H. D. Holmgren, *ibid.* **19**, 698 (1979); V. E. Viola, Nucl. Phys. **A471**, 53c (1987); R. E. L. Green *et al.*, Phys. Rev. C **35**, 1341 (1987).
[2] For reviews see D. H. Boal, Adv. Nucl. Phys. **15**, 85 (1984); W. A. Lynch, Annu. Rev. Nucl. Sci. **37**, 493 (1987).
[3] R. E. L. Green and R. A. Korteling, Phys. Rev. C **22**, 1594 (1980).

[4] R. Korteling, in *Nuclear Dynanics and Nuclear Disassembly,* Proceedings of the American Chemical Society, edited by J. B. Natowitz (World Scientific, Dallas, 1989), p. 125.
[5] B. M. K. Nefkens, in *International Research Facilities,* Proceedings of the European Physical Society and the Ruđer Bošković Institute, edited by I. Šlaus (European Physical Society, ZIRS Zagreb, 1989).
[6] J. Berger *et al.*, Phys. Rev. Lett. **61**, 919 (1988).
[7] B. Zeidman, LANL Report LA-4773-Ms, 1971.
[8] G. S. Blanpied, LANL Report LA-7262-T, 1978.
[9] J. P. Alard *et al.*, Nuovo Cimento A **30**, 320 (1975).
[10] D. H. Boal *et al.*, Phys. Rev. C **23**, 2788 (1981); F. Hachenberg *et al.*, Phys. Lett. **97B**, 183 (1980).
[11] D. R. F. Cochran *et al.*, Phys. Rev. D **6**, 3085 (1972).

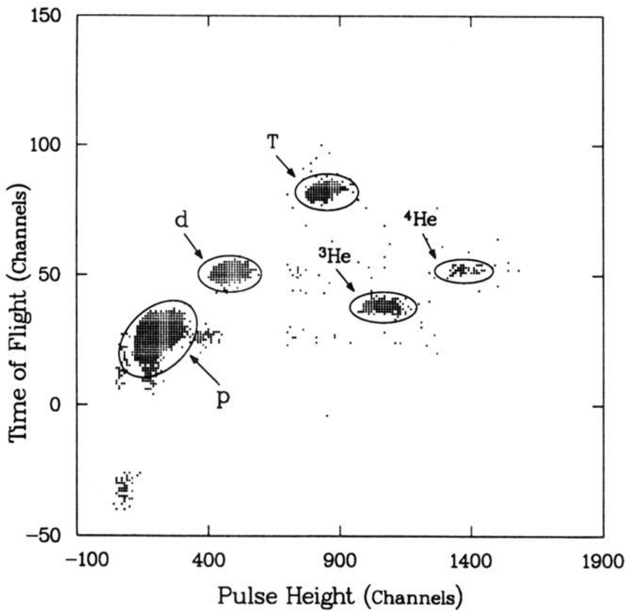

FIG. 1. Two-parameter particle identification spectrum based on time of flight and pulse height.